Journal of Cellular Biochemistry 62:383–396 (1996)

Filamin Translocation is an Early Endothelial Cell Inflammatory Response to Bradykinin: Regulation by Calcium, Protein Kinases, and Protein Phosphatases

Qin Wang, Wayne F. Patton, Eddie T. Chiang, Herbert B. Hechtman, and David Shepro

Microvascular Research Laboratory, Biological Science Center and Center for Photonics Research, Boston University, Boston, Massachusetts 02215 (Q.W., W.F.P., E.T.C., D.S.), and Department of Surgery, Harvard Medical School, Boston, Massachusetts 02214 (H.B.H.)

Abstract Endothelial cell (EC) cytoskeletal proteins are one of the earliest primary targets of second messenger cascades generated in response to inflammatory agonists. Actin binding proteins, by modulating actin gelation-solation state and membrane-cytoskeleton interactions, in part regulate cell motility and cell-cell apposition. This in turn can also modulate interendothelial junctional diameter and permeability. Nonmuscle filamin (ABP-280), a dimeric actin-crosslinking protein, promotes orthogonal branching of F-actin and links microfilaments to membrane glycoproteins. In the present study, immunoblot analysis demonstrates that filamin protein levels are low in sparse EC cultures, increase once cell-cell contact is initiated and then decrease slightly at post-confluency. Both bradykinin and ionomycin cause filamin redistribution from the peripheral cell border to the cytosol of confluent EC. Forskolin, an activator of adenylate cyclase, blocks filamin translocation. Bradykinin activation of EC is not accompanied by significant proteolytic cleavage of filamin. Instead, intact filamin is recycled back to the membrane within 5–10 min of bradykinin stimulation. Inhibitors of calcium/calmodulin dependent protein kinase (KT-5926 and KN-62) attenuate bradykinin-induced filamin translocation. H-89, an inhibitor of cAMP-dependent protein kinase, causes translocation of filamin in unstimulated cells. Calyculin A, an inhibitor of protein phosphatases, also causes translocation of filamin in the absence of an inflammatory agent. ML-7, an inhibitor of myosin light chain kinase and phorbol myristate acetate, an activator of protein kinase C, do not cause filamin movement into the cytosol, indicating that these pathways do not modulate the translocation. Pharmacological data suggest that filamin translocation is initiated by the calcium/calmodulin-dependent protein kinase whereas the cAMP-dependent protein kinase pathway prevents translocation. Inflammatory agents therefore may increase vascular junctional permeability by increasing cytoplasmic calcium, which disassembles the microfilament dense peripheral band by releasing filamin from F-actin.

Key words: actin, bradykinin, filamin, phosphatase, kinase, permeability

Paracellular channels, non-junctional channels, endocytotic vesicles, fenestrae, and pumps are specialized modes of transport that account for the selective permeability and barrier functions of different microvascular beds [Shepro, 1988; Renkin, 1988; Rippe and Haraldsson, 1994]. The regulation of these structures principally account for moment to moment changes in exchange between the intravascular and interstitial fluid compartments. The interendothelial junction forms the primary route for the passage of fluid and solutes, as well as the transmigration of cells, between the intravascular compartment and interstitium [Majno et al., 1969; Palade et al., 1991; Mineau-Hanschke et al., 1989, 1990; McDonald, 1994; Shepro, 1994; Rippe and Haraldsson, 1994]. EC motility has long been thought to play a direct role in vascular permeability changes accompanying the transition from a healthy to diseased state

Abbreviations used: cAMP, adenosine 3′-5′-cyclic monophosphate; IP_3, inositol 1,4,5-triphosphate; Ca^{2+}, calcium; CaM-PK II, calcium/calmodulin dependent protein kinase; cAMP-PK, cAMP-dependent protein kinase; MLCK, myosin light chain kinase; PKC, protein kinase C; EC, endothelial cell; EDTA, ethylenediaminetetraacetic acid; EGTA, ethylene glycol-bis (β-amino-ethyl ether) N,N,N′N′-tetra acetic acid, PMSF, phenylmethylsulfonyl fluoride; DDF, differential detergent fractionation; IBMX, 1-methyl-3-isobutylxanthine; PIPES, 1,4-Piperazine bis-(ethanesulfonic acid).

Received January 4, 1996; accepted February 26, 1996.

Address reprint requests to Wayne F. Patton, Ph.D., Microvascular Research Laboratory, Biological Science Center and Center for Photonics Research, Boston University, 5 Cummington Street, Boston, MA 02215.

[Metchnikoff, 1897, 1968; Krogh, 1922]. Pathophysiological transport arising from local tissue injury results from the unregulated opening of postcapillary venules and capillary junctions [Shepro, 1988; Lum and Malik, 1994]. It is our contention that pores are dynamic channels of varying radii regulated in part by changes in the cytoskeleton. Normal paracellular permeability is regulated in part by metabolites produced locally by EC and extramural cells (smooth muscle, pericytes) in combination with blood-delivered paracrine secretions [Shepro, 1988]. Exaggerated secretion of these auto-regulatory metabolites into the circulation leads to a pathophysiological setting of unregulated junctional *permeability, non-cardiogenic inflammatory edema.* However, the specific complement of EC cytoskeletal proteins involved in regulating vasopermeability are not known.

The vasoactive, nine-residue peptide hormone bradykinin is a regulatory metabolite that modulates vasodilation, increases vasopermeability and produces pain [Lewis, 1986]. These effects represent three of the cardinal signs of early stages of inflammation (erythema, edema, and pain). Bradykinin is produced in human plasma by a cascade consisting of three pre-enzyme-enzyme transformations and represents the major final biologically active product of the kallikrein-kinin pathway. The kinin is rapidly degraded by a number of peptidases, especially angiotensin converting enzyme, on the EC surface [Yong et al., 1992]. Angiotensin converting enzyme inhibitors potentiate the dilator response to bradykinin in coronary microcirculation [Hecker et al., 1994]. In EC, bradykinin increases intracellular calcium (Ca^{2+}) concentration, stimulates arachidonic acid release, and initiates the production of nitric oxide (NO) and prostacyclin (PGI_2) [Mombouli and Vanhoutte, 1995]. The actions of bradykinin are mediated by specific G-protein-coupled receptors possessing seven transmembrane domains. The two classes of bradykinin receptors (B1, B2) differ in their affinities for bradykinin and responsiveness to specific agonists and antagonists [Steranka et al., 1989]. Endothelial cells have both B1 and B2 receptors [Smith et al., 1995]. Bradykinin binds to the B2 receptor with higher affinity than other related kinin metabolites such as $desArg^9$ bradykinin. Bradykinin association with the B2 receptor activates phospholipase C which in turn leads to the generation of inositol 1,4,5-triphosphate (IP_3) and sn-1,2-diacyl glycerol (DAG) [Smith et al., 1995]. IP_3 induces release of Ca^{2+} from intracellular stores in the endoplasmic reticulum, followed by a secondary elevation of Ca^{2+} levels due to the influx of extracellular Ca^{2+}. This in turn leads to activation of Ca^{2+}/calmodulin-dependent protein kinase (CaM-PK II). DAG activates the protein kinase C (PKC) pathway.

Proteins at the membrane-cytoskeleton interface coordinate a number of interactions critical to the maintenance of EC barrier function, which include cytoplasmic responses to external stimuli, cell motility, and cell-cell attachments [Gottlieb et al., 1991; Luna and Hitt, 1992]. We believe these proteins are key substrates of inflammatory second messenger cascades produced by agents like bradykinin. The primary mode of attaching actin filaments to the platelet plasma membrane is via nonmuscle filamin (also referred to as actin-binding protein or ABP-280) [Weihing, 1985]. Similar membrane-cytoskeleton linkages may also be operative in EC. Studies evaluating EC surface reactivity to over 1000 monoclonal antibodies, raised against a variety of leukocyte antigens, reveal a relatively high degree of homology between the EC surface and that of the platelets [Favaloro et al., 1990]. Nonmuscle filamin orchestrates the association of cytoskeletal actin with the plasma membrane via the platelet glycoprotein GP1b [Fox, 1985; Okita et al., 1985; Ohta et al., 1991]. Platelet GP1b is also present in human umbilical vein EC [Asch et al., 1988; Sprandio et al., 1988; Konkle et al., 1990]. This nonintegrin adhesion molecule binds von Willebrand factor and mediates adhesion of platelets to injured blood vessels [Pavalko and Otey, 1994]. Filamin plays a key role in stabilizing membrane-cytoskeletal interactions in a variety of eukaryotic cells [Hartwig et al., 1991]. Melanoma cell lines with normal levels of gelsolin, α-actininin, profilin, and fodrin, but lacking filamin display extensive, continuous blebbing of the plasma membrane [Cunningham et al., 1992]. Transfection of filamin into the deficient cell lines prevents the uncontrolled blebbing behavior.

Cytoskeletal proteins are primary targets of second messenger phosphorylation cascades. Ankyrin, for instance, has over 220 predicted sites for phosphorylation by protein kinases [Chan et al., 1993]. Analysis of nonmuscle filamin sequence data reveals 380 serine/threonine residues including nine calcium-calmodulin dependent protein kinase, 13 cAMP-dependent protein

kinase, 30 casein kinase II, 33 protein kinase C, and 36 MAP kinase consensus phosphorylation sites [Gorlin et al., 1990]. Four phosphorylated forms of nonmuscle filamin, containing 18 to 40 moles phosphate per monomer, have been purified from resting platelets [Wu et al., 1994].

This study evaluates functional changes in filamin distribution arising from bradykinin-induced EC inflammatory second messenger pathways. Filamin expression increases substantially when cultured EC reach confluency, principally localizing at regions of cell-cell contact. Filamin rapidly and reversibly translocates from the EC plasma membrane to the cytosol within 20 s of exposure to bradykinin. The translocation coincides with the initial, transient calcium peak generated by bradykinin. Translocation is mediated by the calcium/calmodulin dependent protein kinase (CaM-PK II) signaling pathway, while the cAMP-dependent protein kinase (cAMP-PK) signaling pathway blocks translocation. These observations coupled with our and other investigators' data that bradykinin increases microvascular junctional patency suggest that filamin translocation is an early step that precedes the loss of intravascular fluid and macromolecules to the interstitial space.

MATERIALS AND METHODS

Materials

Ionomycin, KT 5926, KN-62, ML-7, and Fura-2/AM are obtained from Calbiochem (La Jolla, CA, USA). Forskolin, 1,9-dideoxy forskolin, phorbol 12-myristate, 4α-phorbol 12-myristate, H-89, okadaic acid, calyculin A, and calpeptin are obtained from LC laboratory (Woburn, MA, USA). Bradykinin, IBMX and calpain are obtained from Sigma (St. Louis, MO, USA).

Endothelial Cell Isolation and Cultivation

Bovine pulmonary artery EC are isolated as previously described [Shepro et al., 1974; Mineau-Hanschke et al., 1990]. Pulmonary arteries are obtained from a local slaughter house and EC are removed by gentle scraping with forceps of the exposed lumen of dissected vessels. After incubation in 0.1% collagenase in phosphate buffered saline (PBS) for 15 min at 37°C, the cells are centrifuged at 2000 rpm for 4 min, resuspended in Dulbecco's modified Eagle's medium (DMEM) containing 20% bovine calf serum (BCS), penicillin (100 U/ml), streptomycin (100 μg/ml), L-arginine (1 mM), L-glutamine (2 mM), and seeded onto six-well plates at a density of two arteries per plate. This corresponds to approximately 7.5×10^4 cells per plate. 1 week later, the cells are refed with 7% BCS. Cells are subsequently refed every 2–3 days and sub-passaged by trypinization as necessary. All experiments are performed with passage 4–10 cells.

Preparation of Cell Lysates and Subcellular Fractions

EC seeded onto 100 mm culture dishes are rinsed twice in PBS (Ca^{2+}/Mg^{2+}-free), and lysed by adding 100°C sample buffer I containing 2.5% sodium dodecyl sulfate (SDS), 200 mM DTT in 10 mM Tris, pH 8.0, and protease inhibitors (5 mM ethylene glycol-bis(β-amino-ethyl ether) N,N,N′N′-tetra acetic acid (EGTA), 1 μg/ml leupeptin, 1 mM phenylmethylsulfonyl fluoride (PMSF), and 0.11 I U aprotinin). The lysate is allowed to cool on ice. Chilled sample buffer II containing 1 mg/ml DNase I and 0.25 mg/ml RNase A is added to the culture dish and the lysate is incubated on ice for an additional 5 min. The cell lysate is collected using an automated pipette, precipitated in ice-cold acetone (final concentration 80%) and redissolved in sample buffer I.

EC are fractionated into cytosol, membrane/organelle, nucleus, and cytoskeleton fractions as previously described [Ramsby et al., 1994]. Briefly, EC seeded onto 100-mm culture dishes are rinsed twice with PBS (Ca^{2+}/Mg^{2+} free) and extracted in ice-cold digitonin buffer (0.01% digitonin, 10 mM PIPES, pH 6.8, 300 mM sucrose, 100 mM NaCl, 3 mM $MgCl_2$, 10 μg/ml phalloidin and protease inhibitors). The cells are incubated on ice with gentle agitation for 10 min. The supernatant (cytosolic fraction) is collected and the residual cell components are sequentially extracted in Triton X-100, Tween-40/deoxycholate, and then SDS. Triton X-100 extraction is performed for 30 min in 0.5% Triton X-100, 10 mM PIPES, pH 7.4, 300 mM sucrose, 100 mM NaCl, 3 mM $MgCl_2$, 3 mM EGTA, protease inhibitors, and 10 μg/ml phalloidin. After the supernatant (membrane/organelle fraction) is collected, the residual material is extracted on ice for 10 min with a Tween-40/deoxycholate buffer, containing 1% Tween 40, 0.5% deoxycholate, 10 mM PIPES, pH 7.4, and protease inhibitors. The supernatant (nuclear fraction) is collected, and hot (100°C) SDS buffer containing 2.5% SDS in 10 mM tris-HCl, pH 8,

200 mM DTT and protease inhibitors, is added to solubilize the cytoskeleton fraction. The culture dish is scraped and chilled on ice. 50 μl sample buffer II (as described in whole cell lysate preparation) is added and the dish is incubated on ice for 5 min. The cytoskeletal fraction is collected and heated at 100°C for 5 min. All subcellular fractions are then acetone-precipitated and redissolved in equal volumes of sample buffer I (as described for the cell lysate extraction).

Evaluation of Subcellular Compartments

Differential detergent fractionation (DDF) is a simple procedure that utilizes various detergents and buffers to isolate subcellular organelles [Ramsby et al., 1994]. Unlike conventional centrifugation procedures, DDF is rapid, preserves cytoskeletal integrity, and can be used with limited quantities of tissue or cells. DDF partitions cells into cytosol, membrane/organelle, nuclear, and cytoskeleton fractions. The cytosolic enzyme marker, lactate dehydrogenase, is assessed by monitoring the conversion of NADH to NAD spectrophotometrically at 340 nm, as previously described [Storrie and Madden, 1990]. The reaction rate is determined as the change in absorbance per min. The plasma membrane marker, alkaline phosphatase, is measured spectrophotometrically using *P*-nitrophenyl phosphate as substrate [Clark and Switzer, 1977]. The absorbance of the released *P*-nitrophenol is monitored at 405 nm. Similarly, the lysosomal markers β-Galactosidase and N-Acetyl-β-D-Glucosaminidase are monitored using *P*-nitrophenyl-β-D-galactopyranoside and *P*-nitrophenyl-β-D-glucosamine as substrates [Findlay et al., 1958; Storrie and Madden, 1990]. DNA distribution is determined by incubating cells in 2 μCi/ml of [^{3}H]-thymidine for 17 h, and monitoring trichloroacetic acid precipitable incorporation in the subcellular fractions by liquid scintillation counting. The cytoskeletal markers; actin, vimentin and myosin heavy chain are monitored by conventional SDS-polyacrylamide gel electrophoresis [Laemmli, 1970].

Electrophoresis, Immunoblotting, and Protein Quantification

Cell extracts, dissolved in sample buffer, are subjected to SDS-polyacrylamide gel electrophoresis using 4–15% gradient gels (Pharmacia, Piscataway, NJ, USA) according to manufacturer's protocol. Equal volume or equal amount of protein are loaded in each lane, depending upon the experiment. Protein is quantified using the BCA protein assay (Pierce, Rockford, IL, USA). After electrophoresis, proteins are electroblotted for 1 h to 0.4 μm pore size nitrocellulose membrane (BioRad, Hercules, CA, USA) using the Pharmacia Phast system [Towbin et al., 1979]. Alternatively, subcellular fractions are applied directly to nitrocellulose using a Bio-Dot SF vacuum apparatus (Bio-Rad Laboratories, Hercules, CA, USA) according to the manufacturer's instructions. After electroblotting or slot-blotting, the membrane is incubated in blocking buffer containing 5% BSA, 0.1% Tween-20 for at least 1 h, followed by incubation in 1:250 dilution of mouse anti-human nonmuscle filamin antibody (Chemicon, Temecula, CA, USA) overnight. The membrane is then incubated in alkaline phosphatase-conjugated goat anti-mouse IgG (Cappel, Durham, NC, USA) and filamin bands are visualized using a nitroblue tetrazolium/5-bromo-4-chloro-3—indoylphosphate *P*-toluidine chromagen system (Sigma, St Louis, MO, USA).

Electroblots are subsequently scanned at 300 dots per inch (dpi) resolution with 256 gray scale levels using a flat-bed scanner interfaced to an Apple Macintosh Power PC microcomputer. Proteins are quantified using NIH Image, a public domain graphics program developed by Dr. W. Rasband, Research Services Branch, NIMH (wayne@helix.nih.gov).

Immunofluorescence Microscopy

EC seeded onto coverslips are rinsed three times with PBS (Ca^{2+}/Mg^{2+} free) and fixed in 3.7% formaldehyde for 10 min at room temperature. After rinsing the cells three times in PBS (Ca^{2+}/Mg^{2+} free), the cells are permeabilised in 0.2% Triton X-100 for 10 min at room temperature, followed by incubation in PBS solution containing 1% normal goat serum and 1% BSA for 30 min. The cells are incubated in 1:50 to 1:200 dilution of mouse anti-human filamin monoclonal antibody (Chemicon, Temecula, CA, USA) for 1 h, followed by three 15 min incubations in PBS containing 1% BSA, 0.1% normal goat serum. The cells are incubated in 1:50 dilution of rhodamine-conjugated goat anti-mouse IgG for 1 h in the dark, and rinsed three times with PBS. The excitation and emission wavelengths of rhodamine are 557 and 580 nm, respectively. The coverslips are mounted on slides in glycerol: H_2O (9:1) and sealed with nail

varnish. The slides are monitored under an inverted IM-35 Zeiss fluorescent microscope.

Intracellular Calcium Measurement

EC are seeded onto glass coverslips and allowed to grow to confluency. Cells are incubated in media containing 8 μM Fura-2/AM for 30 min at 37°C. They are washed three times with physiological saline solution containing 150 mM NaCl, 5 mM KCl, 1.8 mM $CaCl_2$, 5 mM glucose, 1 mM $MgCl_2$, 10 mM HEPES, pH 7.4. The coverslip is transferred into a cell holder and placed into a quartz cuvette. Fluorescence is measured using a Perkin-Elmer LS-50 spectrometer (Perkin-Elmer, Bukinghamshire, England). A water bath is used to maintain the temperature at 37°C. The cells are allowed to equilibrate in the cuvette for 10 min. The excitation wavelength alternates between 340 nm and 380 nm with the emission wavelength fixed at 510 nm. For calibration, 10 μM ionomycin is added, followed by the addition of 5 mM EGTA. The intracellular free Ca^{2+} is calculated from the ratio of the 340/380 nm-induced emission at 510 nm as described [Weintraub et al., 1992].

RESULTS

Subcellular Distribution of Filamin

Changes in the subcellular distribution of filamin are evaluated by differential detergent fractionation (DDF) and immunofluorescence microscopy. While filamin distributional changes are readily apparent by immunofluorescence microscopy, the amount of filamin in different subcellular compartments is better quantified by DDF. This subcellular fractionation technique has previously been validated in hepatocytes using seven marker enzymes, 11 cytoskeletal, and 21 non-cytoskeletal protein markers [Ramsby et al., 1994]. The subcellular distribution of marker enzymes and endothelial cytoskeletal proteins are shown in Table I. Lactate dehydrogenase, a marker of the soluble cytosol is recovered in the cytosol fraction with significant residual activity also found in the membrane/organelle fraction. The majority of lysosomal activity (β-galactosidase and N-acetyl-β-D-glucosaminidase) is found in the membrane/organelle fraction. Alkaline phosphatase is found in both the membrane/organelle fraction and the cytoskeleton fraction. Glycosylphosphatidylinositol (GPI)-anchored proteins, such as alkaline phosphatase, are known to be poorly solubilized from cell membranes by nonionic detergents due to association with detergent-resistant membranes rich in cholesterol and sphingolipids [Schroeder et al., 1994]. DNA, a large macromolecule that is not solubilized by the detergents, is expected to remain in the residual cytoskeletal fraction. Measurement of incorporated tritiated thymidine verifies that the DNA is present in this fraction. Densitometric analysis of SDS-polyacrylamide gels demonstrates that the cytoskeletal proteins, myosin heavy chain, and vimentin are substantially enriched in the cytoskeleton fraction.

Probing electroblotted proteins with monoclonal antibodies specific to nonmuscle and smooth muscle filamin reveals that bovine pulmonary artery EC only express nonmuscle filamin (ABP-280). The nonmuscle filamin-specific antibody reacts exclusively with a single 250 kDa protein

TABLE I. Marker Protein Profile of Endothelial Cell Subcellular Fractions*

Marker	Digitonin/EDTA (cytosolic)	Triton/EDTA (membrane-organelle)	Tween/DOC (nuclear-associated)	Detergent-resistant (cytoskeletal-matrix)
Lactate dehydrogenase	63.7 ± 4.4	25.3 ± 5.2	8.4 ± 1.3	2.6 ± 1.8
β-Galactosidase	1.1 ± 1.7	71.4 ± 7.0	17.5 ± 5.4	10.0 ± 3.7
N-Acetyl-β-Glucosaminidase	2.5 ± 1.1	64.9 ± 2.7	27.3 ± 1.7	4.8 ± 1.4
Alkaline phosphatase	5.5 ± 2.1	29.3 ± 3.7	6.3 ± 1.6	48.6 ± 4.9
Tritiated thimidine incorporation	3.2 ± 2.4	10.0 ± 3.0	3.7 ± 0.4	83.0 ± 5.7
Myosin heavy chain (205 KD)	21.1 ± 4.1	21.0 ± 5.6	6.1 ± 3.3	52.0 ± 5.2
Vimentin (57 kD)	5.5 ± 4.4	3.4 ± 1.9	1.8 ± 0.8	89.3 ± 4.8
Actin (42 kD)	30.0 ± 4.9	15.1 ± 6.2	6.0 ± 4.2	24.0 ± 8.0

*Endothelial cells were isolated by differential detergent fractionation (DDF). Enzymes and proteins are quantified as described in Materials and Methods and normalized to total cellular activity (100%). Data is presented as mean values ± standard deviations ($n \geq 3$).

in EC cell lysates. Evaluation of the subcellular distribution of filamin using DDF indicates that this cytoskeletal protein is found in the membrane/organelle, cytoskeleton and cytosol fractions. Actin, itself, is also distributed between these three compartments (Table I) [Ramsby et al., 1994].

The total amount and subcellular distribution of filamin changes with EC confluency state. EC are seeded at various densities to achieve sparse, preconfluent, confluent, and postconfluent cultures. Immunofluorescence microscopy indicates that filamin is primarily associated with the cell periphery in post-confluent EC, whereas in sparse cultures filamin is found associated with the cytoplasmic stress fibers (data not shown). Filamin protein levels are low in sparse cultures, increase 2.7 and 3 fold in preconfluent and confluent cultures respectively, then decline slightly to 1.5 fold after postconfluence (Fig. 1A). Actin and myosin heavy chain protein levels are unaltered by culture confluency state. Filamin locates primarily in the membrane and cytoskeleton fractions in confluent EC, while in sparse cultures, less filamin is recovered in the membrane fraction (Fig. 1B). The observed changes in the filamin to actin ratio suggest altered cytoplasmic gelation-solation state may accompany the initiation of cell-cell contact. Increasing the filamin to actin ratio is expected to generate a progressively crosslinked cytoplasm.

Ionomycin- and Bradykinin-Induced Filamin Translocation

Both bradykinin and ionomycin cause filamin redistribution from the plasma membrane to the cytosol in confluent EC, as determined by immunofluorescence microscopy (Fig. 2). Immunofluorescence staining reveals filamin is prominently concentrated in the lateral margins of postconfluent EC, at regions of cell-cell contact. Substantial amounts of filamin also co-localize with F-actin stress fibers in the cytoplasm (data not shown). Cytoplasmic filamin localization is predominant in ionomycin- and bradykinin-treated EC, with little or no staining at regions of cell-cell contact (Fig. 2). These observations support the premise that upon exposure of EC to inflammatory mediators, filamin dissociates from the membrane cytoskeleton and redistributes to the cytoplasm. Filamin is observed to return to the lateral margins of bradykinin-treated EC after 5–10 min (Fig. 2E).

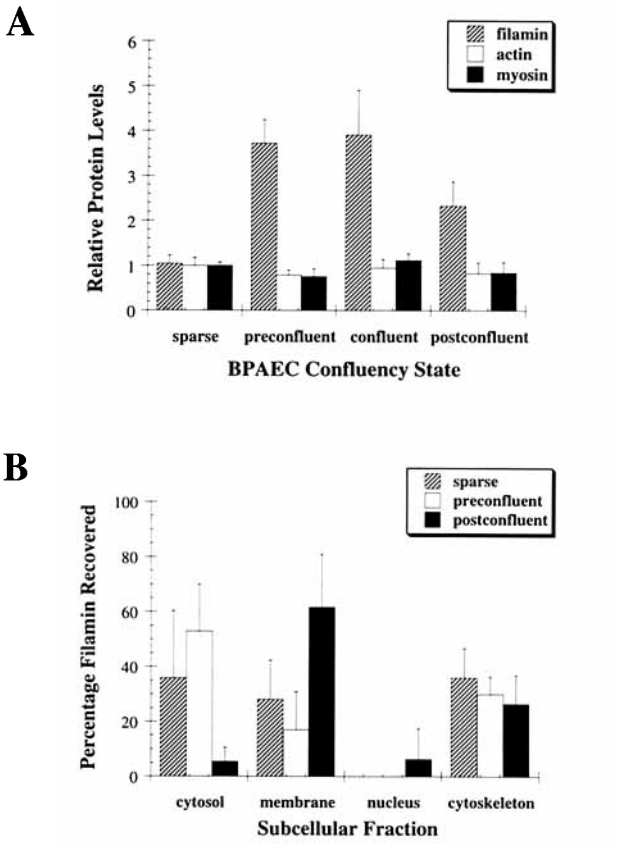

Fig. 1. Changes in filamin expression levels and subcellular distribution as a function of endothelial cell (EC) confluency. **A:** Filamin, actin, and myosin heavy chain protein levels in sparse (95 cells/mm^2), preconfluent (380 cells/mm^2), confluent (800 cells/mm^2), and postconfluent (800 cells/mm^2) EC. Individual proteins are normalized to total protein amount and expressed relative to amounts present in sparse EC. Actin and myosin content were quantified by scanning Coomassie-Blue stained SDS-polyacrylamide gels. Filamin was quantified by scanning immunoblots. Hatched bars: filamin; white bars: actin; black bars: myosin heavy chain. **B:** Subcellular distribution of filamin in sparse, preconfluent, and postconfluent EC. Data is presented as the percentage of filamin in each fraction. Hatched bars: sparse EC; white bars: preconfluent EC; black bars: postconfluent EC. Error bars are means ± standard deviation (n = 3 separate experiments).

In post-confluent EC, 62% and 27% of the filamin is associated with the membrane/organelle and cytoskeleton fractions respectively, whereas 5% is in the cytosol (Fig. 3). Following 1 μM ionomycin treatment for 2 min, 37% of the filamin is present in the membrane/organelle fraction, 22% is associated with the cytoskeleton fraction, and 35% with the cytosol fraction. We consistently observe that filamin translocation involves redistribution between the membrane/organelle and cytosol compartments, with filamin levels in the cytoskeletal compartment re-

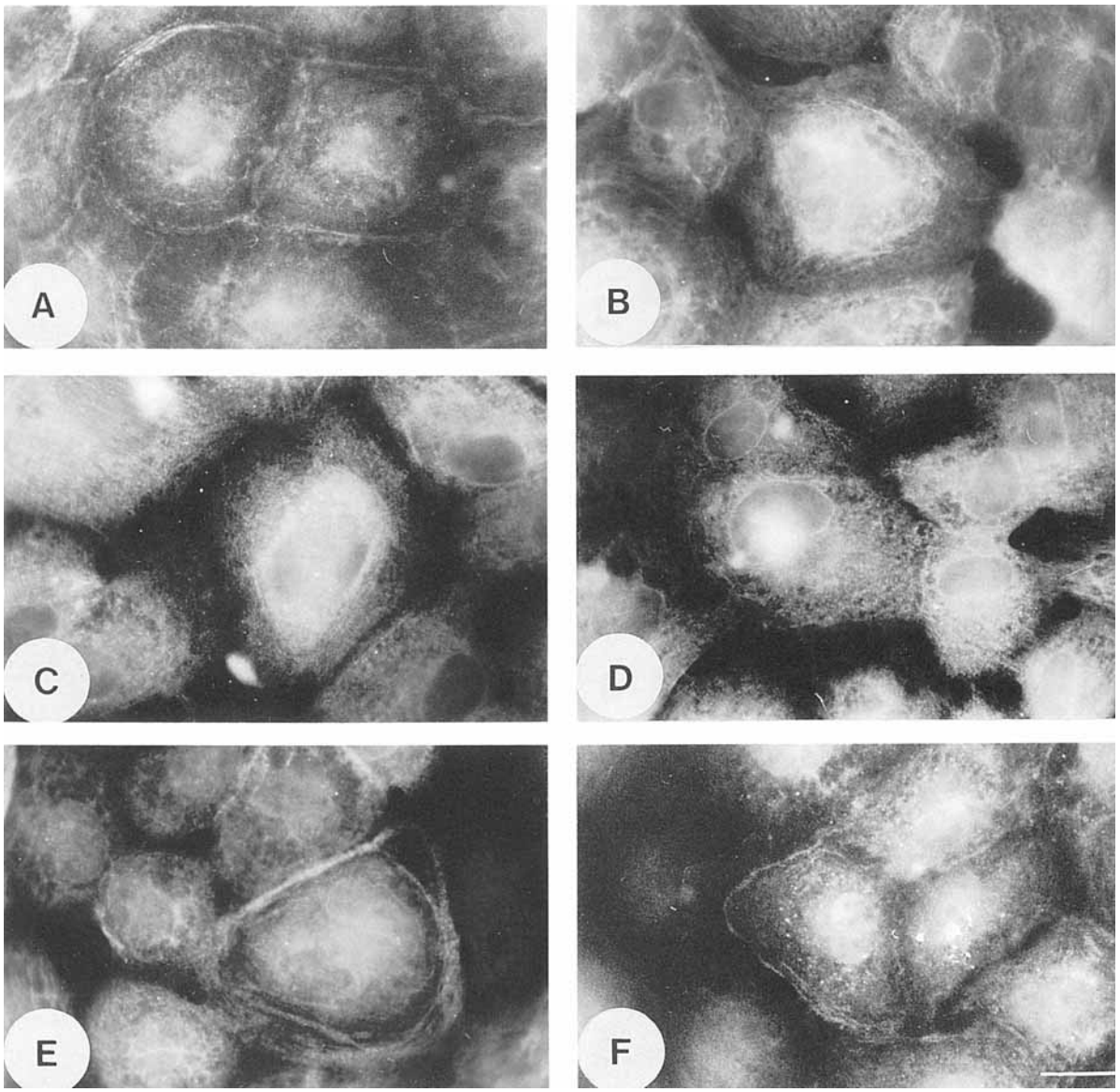

Fig. 2. Subcellular localization of filamin by immunofluorescence microscopy. **A:** Control cells. **B:** Cells treated with bradykinin for 1 min. **C:** Cells treated with bradykinin for 2 min. **D:** Cells treated with bradykinin for 5 min. **E:** Cells treated with bradykinin for 10 min. **F:** Cells treated with bradykinin for 60 min. Significant paracellular filamin staining is observed in control cells. Ionomycin and bradykinin cause filamin to redistribute cytoplasmically. Scale bar: 10 μm.

maining fairly constant. Forskolin, an activator of adenylate cyclase, in combination with 1-methyl-3-isobutylxanthine (IBMX), a phosphodiesterase inhibitor, blocks ionomycin-mediated filamin translocation to the cytosol (Fig. 3).

Ionomycin increases intracellular calcium levels by selectively increasing plasma membrane ion permeability. Whereas ionomycin causes a sustained elevation in intracellular Ca^{2+}, bradykinin generates a biphasic Ca^{2+} response. A rapid and transient increase in intracellular Ca^{2+} concentration is followed by a more sustained phase of elevated Ca^{2+} levels in bovine pulmonary artery EC (Fig. 4A). Dose-response studies indicate that 10–100 nM bradykinin produce the greatest increase in intracellular Ca^{2+} in cultured pulmonary artery EC (data not shown). Based upon nine experiments, the intracellular Ca^{2+} concentration in unstimulated EC is approximately 151 ± 49 nM. Upon exposure to 10 nM bradykinin, intracellular Ca^{2+} levels start to rise in 21 ± 9 s, and reach a peak value of 660 ± 223 nM within 70 ± 25 s. Ca^{2+} levels then decline to a plateau value of 258 ± 76 nM by

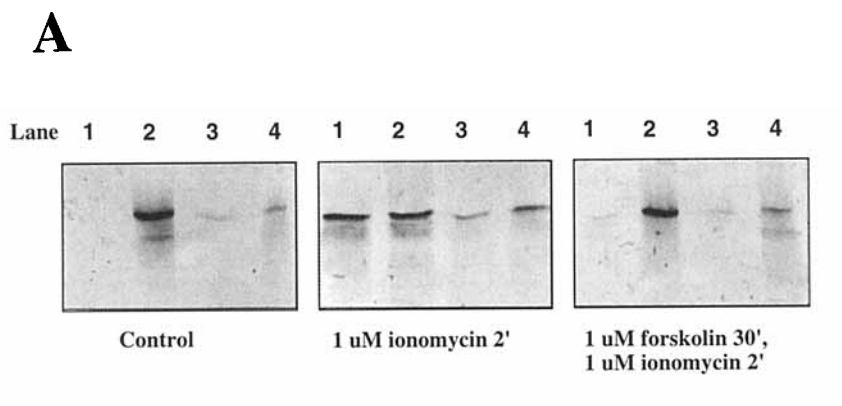

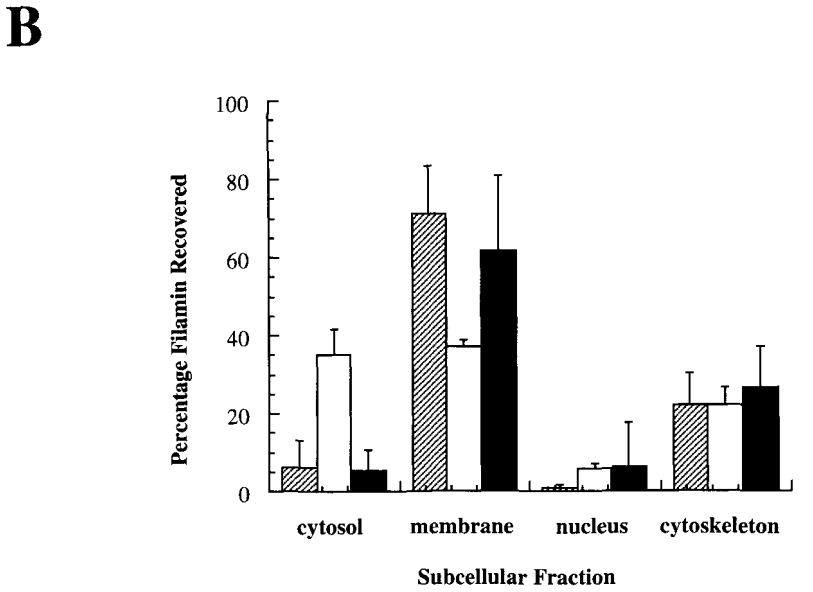

Fig. 3. Subcellular distribution of filamin in control, ionomycin-treated, and forskolin/IBMX pre-treated, ionomycin-treated cells. Cells are separated into four subcellular compartments by differential detergent fractionation. **A:** Electroblotted subcellular fractions are reacted with anti-filamin primary antibody as described in Materials and Methods. *Lanes 1 through 4* correspond to cytosolic, membrane/organelle, nuclear, and cytoskeletal fractions, respectively. **B:** Modulation of ionomycin-induced filamin translocation by forskolin/IBMX. Untreated cells; hatched bars, cells treated with 1 μM ionomycin for 2'; white bars, Cells pretreated with 1 μM forskolin/0.5 mM IBMX for 30 min, followed by 1 μM ionomycin for 2 min; black bars. Error bars are means ± standard deviation (n = 3).

127 ± 24 s, followed by a slow decay to baseline levels after approximately 15 min. This is accompanied by rapid translocation of filamin from the membrane to the cytosol (Fig. 4B). Significant redistribution of filamin is detectable after as little as 20 s exposure to bradykinin, with maximal cytosolic translocation occurring after 2 min exposure. Thus, filamin translocation is temporally correlated with the initial, transient calcium peak. Filamin starts returning to the membrane fraction within 5 min of bradykinin stimulation, during the Ca^{2+} plateau phase.

Filamin Translocation is Dependent Upon Protein Kinase and Phosphatase Pathways

The results obtained with ionomycin stimulation suggest that the CaM-PK II pathway may cause filamin translocation. The ability of forskolin/IBMX to inhibit ionomycin-mediated translocation suggests that the cAMP-PK pathway is

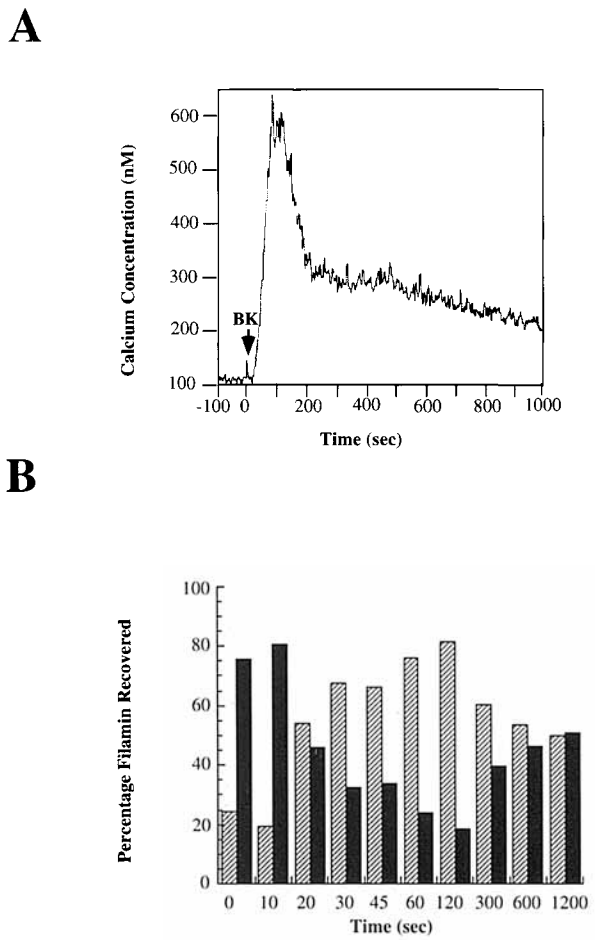

Fig. 4. Time-course of intracellular Ca^{2+} increases and filamin translocation in bradykinin-treated EC. **A:** Representative tracing showing changes in intracellular Ca^{2+} levels in EC treated with 10 nM bradykinin. Cells are preloaded with Fura-2 as described in Materials and Methods. **B:** Representative time-course of filamin translocation in EC treated with 10 nM bradykinin. Cells are exposed to bradykinin for the indicated times and then cytosolic and membrane/organelle compartments are isolated by DDF. Filamin is quantified from slot-blots. Black bars; membrane fraction, hatched bars; cytosol fraction.

important in modulating filamin response to inflammatory signals. This conclusion is supported using a known vasoactive agonist, bradykinin, and pharmacological inhibitors and activators of second messenger pathways. Forskolin/IBMX significantly attenuates bradykinin-induced filamin translocation. The inactive analog, 1,9-dideoxy forskolin does not inhibit bradykinin-induced filamin translocation (data not shown). KT-5926 and KN-62, inhibitors of CaM-PK II, also attenuate bradykinin-induced filamin translocation (Fig. 5A–C). The myosin light chain kinase (MLCK) inhibitor, ML-7, however, is ineffective at preventing filamin translocation (Fig. 5D). H-89, an inhibitor of cAMP-PK, causes translocation of filamin in the absence of an inflammatory agent (Fig. 6A). Spectrometric measurements using Fura-2 indicate that addition of H-89 to EC does not generate a Ca^{2+} peak (data not shown). Phorbol 12-myristate acetate and its inactive analog 4α-phorbol 12-myristate have no effect on filamin translocation in resting cells, which indicates that protein kinase C (PKC) does not play a direct role in filamin translocation (Fig. 6B). Calyculin A, an inhibitor of PP-1 and PP2A serine/threonine protein phosphatases, causes filamin translocation without generating a calcium peak (Fig. 6C). Another PP-1 and PP-2A phosphatase inhibitor, okadaic acid (1 μM), is less effective than calyculin A but also causes filamin translocation in the absence of an inflammatory agent (data not shown).

Bradykinin stimulation of EC is not accompanied by significant proteolytic cleavage of filamin (Fig. 7B). Though we sometimes observe a 190 kDa proteolytic fragment of filamin, especially in the cytoskeletal fraction, the intensity of this band does not increase in time-course experiments using bradykinin. Although filamin is readily cleaved by calpain in vitro (Fig. 7A), calpeptin, a cell permeant calpain inhibitor, does not alter the kinetics of bradykinin-induced filamin translocation (Fig. 7C). Instead, intact filamin is recycled to the membrane after bradykinin stimulation (Fig. 2E–F, Fig. 4B).

DISCUSSION

Since filamin has at least 121 potential protein kinase phosphorylation sites, studying second messenger mediated modification of the protein is a daunting task. Determination of phosphorylation changes in filamin by conventional procedures, such as peptide mapping, amino acid sequencing and in vitro mutagenesis of potential phosphorylation sites, is difficult, especially considering that filamin is a very large protein containing 2,647 amino acids, 380 of which are serines and threonines. Thus, we have opted to use a pharmacological approach initially to examine second messenger-mediated distributional changes in filamin. Utilization of a battery of specific and effective pharmacological inhibitors and activators of protein kinases permits determination of the second messenger pathways likely to regulate filamin redistribution, using intact cells [Hidaka and Kobayahi,

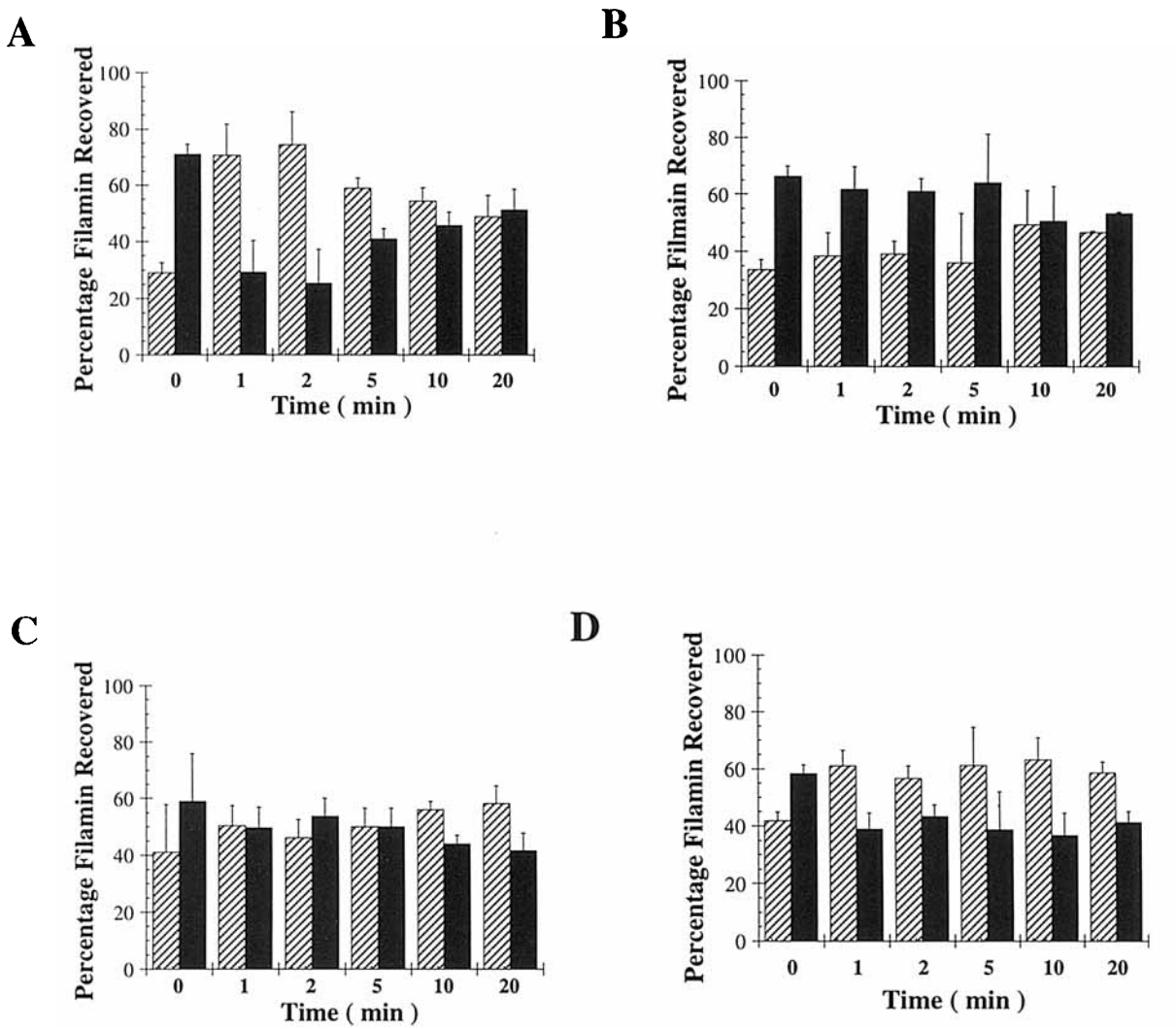

Fig. 5. Modulation of bradykinin-induced filamin translocation. EC are preincubated in culture media, 10 μM KN-62, 5 μM KT-5926 or 5 μM ML-7 for 30 min. Cells are then incubated with 10 nM bradykinin for the indicated times. Membrane/organelle and cytosol compartments are isolated by DDF. **A:** Bradykinin-stimulated control. **B:** Pre-treatment with KN-62, a CaM-PK II inhibitor. **C:** Pre-treatment with KT-5926, another CaM-PK II inhibitor. **D:** Pre-treatment with ML-7, an MLCK inhibitor. Black bars; membrane fraction, hatched bars; cytosol fraction. Error bars are means ± standard deviation (n = 3).

1993]. KT-5926 and KN-62 are respectively four times and 100 times more effective at inhibiting CaM-PK II than MLCK. ML-7 is approximately 70 times more potent at inhibiting MLCK than CAM-PK II. H-89 is 590 times more selective for cAMP-PK than other kinases, while forskolin is well known to increase intracellular cAMP levels by activation of adenylate cyclase. Phorbol myristate acetate is an activator of PKC while okadaic acid and calyculin A are inhibitors of protein phosphatases.

This study demonstrates that filamin association with the membrane cytoskeleton is regulated by CaM-PK II, cAMP-PK, and protein phosphatases. PKC and MLCK second messenger pathways do not appear to regulate filamin redistribution. We further observe that filamin's calpain cleavage site does not appear to play a significant role in bradykinin-mediated inflammatory processes. We find calyculin A and to a lesser extent okadaic acid promote filamin translocation in the absence of an inflammatory stimulus. Both agents are known to inhibit PP2A with equal potency but calyculin A is a more potent inhibitor of PP-1 than okadaic acid. Anti-PP-1 antibody selectively labels the actin microfilament network of rat fibroblasts whereas microinjection of PP-1, but not PP-2A, induces

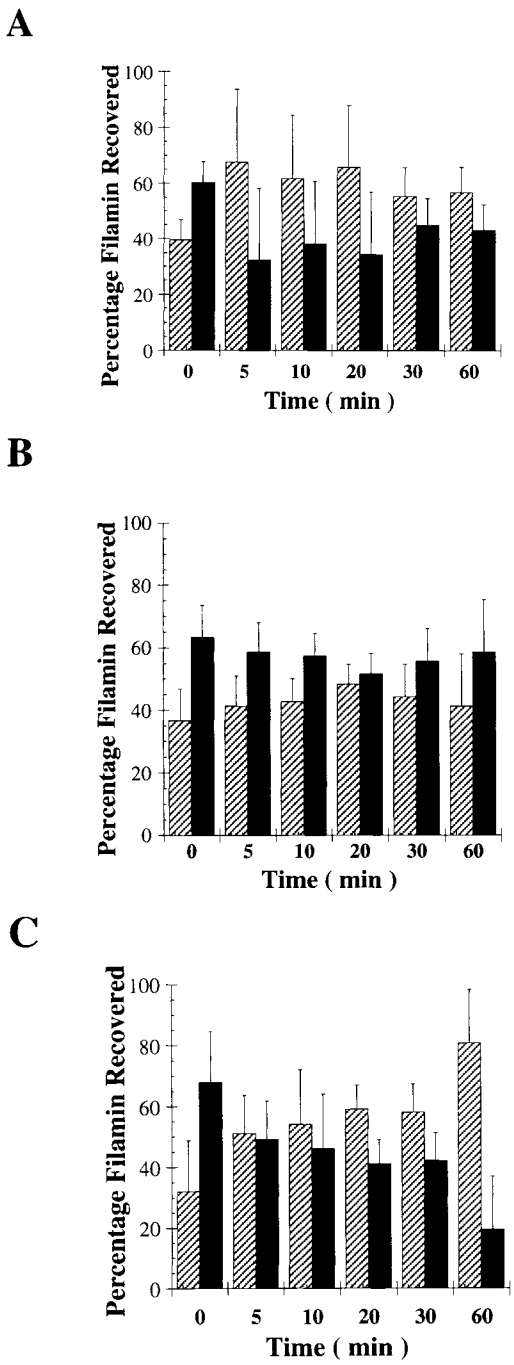

Fig. 6. Regulation of filamin translocation by phosphorylation pathways. EC are incubated with the different activators and inhibitors of second messenger cascades for the indicated times. Membrane/organelle and cytosol compartments are isolated by DDF. **A:** Treatment with 10 μM H-89, a cAMP-PK inhibitor. **B:** Treatment with 5 μM phorbol 12-myristate acetate, a protein kinase C activator. **C:** Treatment with 5 nM calyculin A, a protein phosphatase inhibitor. Black bars; membrane fraction, hatched bars; cytosol fraction. Error bars are means ± standard deviation (n = 3).

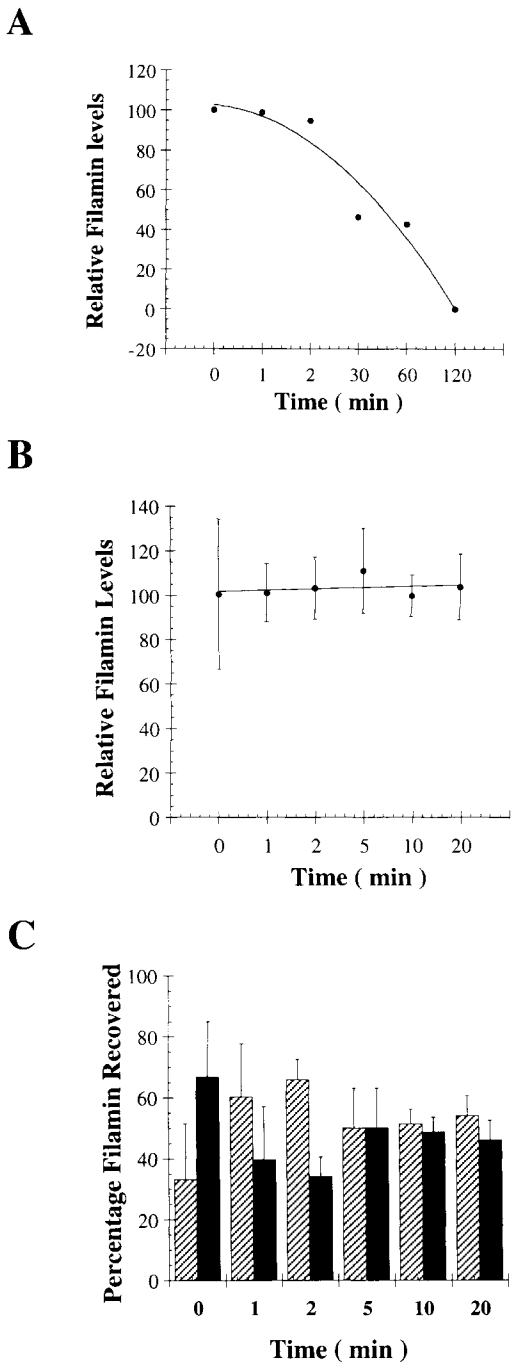

Fig. 7. Evaluation of proteolytic processes during bradykinin-induced filamin redistribution. **A:** In vitro fragmentation of filamin with calpain. **B:** Analysis of filamin levels in bradykinin-stimulated EC. Cells are treated with 10 nM bradykinin for 1, 2, 5, 10, and 20 min. Whole cell lysates are collected and analyzed by Western blotting. Though filamin has a calpain cleavage site, bradykinin does not cause proteolysis. **C:** Calpeptin pre-treatment of bradykinin-stimulated cells. Cells are exposed to 10 μg/ml calpeptin for 5', followed by 10 nM bradykinin treatment for 1', 2', 5', 10', 20'. Membrane/organelle and cytosol compartments are isolated by DDF. Black bars; membrane fraction, hatched bars; cytosol fraction. Error bars are means ± standard deviations (n = 3).

rapid and reversible changes in microfilament organization [Fernandez et al., 1990]. This suggests that PP-1 plays an important role in modulating the actin microfilament network in mammalian cells [Fernandez et al., 1990].

Utilizing aortic EC grown on microcarrier beads we have determined that bradykinin increases permeability to trypan-blue conjugated bovine serum albumin and that phalloidin prevents this increase by stabilizing the actin microfilament network [Alexander et al., 1988]. Moreover, pulmonary microvessel EC grown on silicon rubber contract and wrinkle the substratum within 3–8 min exposure to bradykinin [Morel et al., 1989]. After 10–20 min the process is reversed and wrinkles underneath the cells disappear. Bradykinin-induced increases in intracellular Ca^{2+} may directly regulate vascular barrier function by causing filamin to dissociate from the membrane cytoskeleton. Bradykinin stimulation of bovine pulmonary artery EC causes a rapid increase in intracellular Ca^{2+}, followed by a significant reorganization of microfilaments and cell shape change. The observed time-course for these changes in cultured EC are similar to those documented in vivo. In the hamster cheek pouch model, bradykinin-induced increases in vascular permeability are detectable within 2 min and are maximal by 5 min [Murray et al., 1991]. Other inflammatory agents produce similar changes in cultured EC. For example, after stimulation of pulmonary artery EC with α-thrombin, IP_3 levels increase within 10 s and return to baseline values within 20 s [Lum et al., 1992]. Ca^{2+} is rapidly mobilized, peaking at about 17 s, followed by a second plateau phase of slow decay to half maximal peak height by 51 s. Increases in both IP_3 and Ca^{2+} levels occur before maximal increases in vascular permeability and microfilament rearrangement occur at approximately 2 min. Vascular permeability returns to baseline 15–60 min after exposure to the inflammatory agonist.

Two possible EC cytoskeleton-based mechanisms may account for increased vascular permeability. Vasoactive agonists could decrease EC junctional apposition (retraction model) and/or activate intrinsic contractile activity (contraction model) [Wysolmerski and Lagunoff, 1991; Sheldon et al., 1993]. The two mechanisms are not mutually exclusive. In the contraction model calcium initiates myosin light chain kinase (MLCK) phosphorylation of myosin light chain, which activates the acto-myosin machinery [Wysolmerski and Lagunoff, 1991]. In the retraction model, ECs are tethered to one another at their cell borders and possess a constitutive centripetal tension that is only expressed when tethering is interrupted [Sheldon et al., 1993]. We believe that the EC become untethered when calcium activates the CaM-PK II second messenger pathway which disrupts filamin-plasma membrane glycoprotein interactions.

We propose that filamin regulates EC paracellular permeability by responding to anti- and pro-inflammatory signals. Filamin molecules in the membrane/organelle compartment regulate membrane-cytoskeleton interactions through the dense peripheral band of F-actin. Filamin is known to specifically bind to at least three different transmembrane glycoproteins; platelet GP1bα (CD42b), leukocyte FcγR1 (CD64), and leukocyte β2-integrin (CD18), but the EC glycoproteins filamin associates with are undefined [Fox, 1985; Okita et al., 1985, Ohta et al., 1991; Sharma et al., 1995]. When EC are exposed to an inflammatory agonist, the Ca^{2+}/IP_3 pathway is initiated, leading to activation of the CaM-PK II second messenger pathway and translocation of filamin to the cytosol. It is presently unclear whether CaM-PK II phosphorylates filamin, a plasma membrane protein bound to filamin or some other accessory protein. In vitro, phosphorylation of chicken gizzard filamin by CaM-PK II has been demonstrated to reduce its affinity for actin microfilaments, whereas dephosphorylation with PP2A restores cross-linking activity [Ohta and Hartwig, 1995]. Filamin translocation leads to disassembly of the dense peripheral band and increased paracellular permeability. Ca^{2+}-dependent myosin light chain phosphorylation may potentiate filamin-mediated paracellular leakiness by inducing stress fiber contraction.

Possible mechanisms for restoring barrier function are activation of protein phosphatases, activation of cAMP-PK and/or inhibition of CaM-PK II. Dephosphorylation of filamin, its putative plasma membrane ligand or an accessory protein by phosphatases may allow filamin to reassociate with and reorganize the microfilament network, allowing barrier function to be reestablished. In situ studies using [γ-^{32}P] ATP indicate that cAMP elevating agents, such as PGE_1, directly phosphorylate filamin via cAMP-PK [Chen and Stracher, 1989]. Filamin phosphorylation can be blocked with a synthetic peptide mimicking the active site sequence of

the muscle cAMP-PK inhibitor and by thrombin, an activator of CaM-PK II [Chen and Stracher, 1989]. Agonist-induced vascular permeability increases may be prevented or reversed by cAMP through phosphorylation of the target of CaM-PK II phosphorylation. This may be the mechanism involved in preventing ischemia-reperfusion-induced pulmonary capillary permeability using forskolin and dibutyryl-cAMP [Adkins et al., 1992]. In addition, negative feedback mechanisms involving cAMP may modulate the inflammatory response, causing filamin to recycle back to the membrane-cytoskeleton interface.

In summary, agonists that activate the CaM-PK II pathway cause the rapid and reversible translocation of filamin whereas activators of the cAMP-PK pathway, block the translocation. Filamin translocation is not directly influenced by the MLCK or PKC pathways. Inflammatory agents that increase EC junctional permeability by increasing cytoplasmic calcium, may disassemble the microfilament dense peripheral band by releasing filamin from F-actin.

ACKNOWLEDGMENTS

The authors thank Laurie Hastie, Nancy Chung-Welch, and Michael Lu for useful discussions and careful reading of this manuscript. This project was supported by NIH grants HL-43875 and 48553; GM-24891 and 35141.

REFERENCES

Adkins W, Barnard J, May S, Seibert A, Haynes J, Taylor A (1992): Compounds that increase cAMP prevent ischemia-reperfusion pulmonary capillary injury. J Appl Physiol 72:492–497.

Asch A, Adelman B, Fujimoto M, Nachman R (1988): Identification and isolation of a platelet GP1b-like protein in human umbilical vein endothelial cells and bovine aortic smooth muscle cells. J Clin Invest 81:1600–1607.

Alexander JS, Hechtman HB, Shepro D (1988): Phalloidin enhances endothelial barrier function and reduces inflammatory permeability in vitro. Microvasc Res 35:308–315.

Carson M, Shasby S, Lind S, Shasby M (1992): Histamine, actin-gelsolin binding, and polyphosphoinositides in human umbilical vein endothelial cells. Am J Physiol 263 (Lung Cell Mol Physiol 7):L664–L669.

Chan W, Kordeli E, Bennett V (1993): 440-kD Ankyrin$_B$: Structure of the major developmentally regulated domain and selective localization in unmyelinated axons. J Cell Biol 123:1463–1473.

Chen M, Stracher A (1989): In situ phosphorylation of platelet actin-binding protein by cyclic AMP-dependent protein kinase stabilizes it against proteolysis by calpain. J Biol Chem 264:14282–14289.

Clark JM, Switzer RL (1977): Kinetic characteristics of wheat germ acid phosphatase. In: "Experimental Biochemistry," 2nd ed. San Francisco: W.H. Freeman and Co. pp 105–108.

Cunningham C, Gorlin J, Kwiatkowski D, Hartwig J, Janmey P, Byers H, Stossel T (1992): Actin-binding protein requirement for cortical stability and efficient locomotion. Science 255:325–327.

Favaloro E, Moraitis N, Bradstock K, Koutts J (1990): Co-expression of haemopoietic antigens on vascular endothelial cells: a detailed phenotypic analysis. Br J Haematol 74:385–394.

Fernandez A, Brautigan D, Mumby M, Lamb N (1990): Protein phosphatase type-1, not type-2A, modulates actin microfilament integrity and myosin light chain phosphorylation in living nonmuscle cells. J Cell Biol 111:103–112.

Findlay, Levvy, Marsch (1958): Inhibition of glycosidase by aldonolactones of corresponding configuration. Biochem J 69:467–476.

Fox J (1985): Identification of actin-binding protein as the protein linking the membrane skeleton to glycoproteins on platelet plasma membrane. J Biol Chem 263:13303–13309.

Gorlin J, Yamin R, Egan S, Stewart M, Stossel T, Kwiatkowski D, Hartwig J (1990): Human endothelial actin-binding protein (ABP-280, nonmuscle filamin): A molecular leaf spring. J Cell Biol 111:1089–1105.

Gottlieb A, Langille L, Wong M, Kim D (1991): Biology of disease: Structure and function of the endothelial cytoskeleton. Lab Invest 65:123–137.

Hartwig J, Kwiatkowski D (1991): Actin-binding proteins. Curr Opin Cell Biol 3:87–97.

Hecker M, Porsti I, Bara A, Busse R (1994): Potentiation by ACE inhibitors of the dilator response to bradykinin in the coronary microcirculation: Interaction at the receptor level. Br J Pharmacol 111:238–244.

Hemric M, Tracy P, Haeberle J (1994): Caldesmon enhances the binding of myosin to the cytoskeleton during platelet activation. J Biol Chem 269:4125–4128.

Hidaka H, Kobayashi R (1993): Use of protein (serine/threonine) kinase activators and inhibitors to study protein phosphorylation in intact cells. In Hardie DG (ed): "Protein Phosphorylation. A Practical Approach." New York: IRL Press. pp. 87–107.

Kennelly P, Krebs E (1991): Consensus sequences as substrate specificity determinants for protein kinases and protein phosphatases. J Biol Chem 266:15555–15558.

Konkle B, Shapiro S, Asch A, Nachman R (1990): Cytokine-enhanced expression of glycoprotein 1ba in human endothelium. J Biol Chem 265:19833–19838.

Krogh A (1922): "The Anatomy and Physiology of Capillaries." New Haven: Yale University Press, pp. 47–69.

Laemmli U (1970): Cleavage of structural proteins during the assembly of the head of the bacteriophage T4. Nature 227:680–685.

Lewis G (1986): Mediators of inflammation. Bristol, U.K.: Wright, IOP Publishing, Ltd. pp. 20–22.

Lum H, Malik A (1994): Regulation of vascular endothelial barrier function. Am J Physiol 267 (Lung Cell Mol Physiol 11):L223–L241.

Lum H, Aschner J, Phillips P, Fletcher P, Malik A (1992): Time-course of thrombin-induced increase in endothelial permeability: Relationship to $Ca^{2+}{}_i$ and inositol polyphosphates. Am J Physiol 263 (Lung Cell Mol Physiol 7):L219–L225.

Luna E, Hitt A (1992): Cytoskeleton-plasma membrane interactions. Science 258:955–964.

Majno GS, Shea S, Leventhal M (1969): Endothelial contraction induced by histamine type mediators. An electron microscopic study. J Cell Biol 42:647–672.

McDonald DM (1994): Endothelial gaps and permeability of venules in rat tracheas exposed to inflammatory stimuli. Am J Physiol (Lung Cell Mol Physiol): 266:461–483.

Metchnikoff E (1897): Chapter 9: Endothelium of vessel walls. In: "Lectures of Comparative Pathology of Inflammation." New York: Doner Publications, 135–137.

Mineau-Hanschke R, Hechtman HB, Shepro D (1989): Endothelial cell junctional integrity modulation by serotonin: An ultrastructural analysis. Tissue Cell 21:161–170.

Mineau-Hanschke R, Wiles M, Morel NML, Shepro D (1990): Modulation of cultured pulmonary microvessel and arterial endothelial cell barrier structure and function by serotonin. Microvasc Res 39:140–155.

Mombouli J, Vanhoutte P (1995): Kinins and endothelial control of vascular smooth muscle. Annu Rev Pharmacol Toxicol 35:679–705.

Morel NML, Dodge AB, Patton WF, Herman I (1989): Pulmonary microvascular endothelial contractility on silicon rubber substrate. J Cell Physiol 141:653–659.

Murray M, Heistad D, Mayhan W (1991): Role of protein kinase C in Bradykinin-induced increases in microvascular permeability. Circ Res 68:1340–1348.

Ohta Y, Stossel T, Hartig J (1991): Ligand sensitive binding of actin-binding protein to immunoglobulin G Fc receptor I (FcgRI) Cell 67:275–282.

Ohta Y, Hartwig J (1995): Actin filament cross-linking by chicken gizzard filamin is regulated by phosphorylation in vitro. Biochemistry 34:6745–6754.

Okita L, Pidard D, Newman P, Montgomery R, Kunicki T (1985): On the association of glycoprotein 1b and actin-binding protein in human platelets. J Cell Biol 100:317–321.

Palade GE (1991): "The Lung: Scientific Foundations." Crystal R, West J, Barnes P, Cherniack N, Weibel E (eds). New York: Raven Press.

Pavalko F, Otey C (1994): Role of adhesion molecule cytoplasmic domains in mediating interactions with the cytoskeleton. PSEBM 205:282–293.

Pontremoli S, Melloni E, Michetti M, Sparatore B, Salamino F, Sacco O, Horecker B (1987): Phosphorylation and proteolytic modification of specific cytoskeletal proteins in human neutrophils stimulated by phorbol 12-myristate 13-acetate. Proc Natl Acad Sci USA 84:3604–3608.

Ramsby M, Makowski G, Khairallah E (1994): Differential detergent fractionation of isolated hepatocytes: Biochemical, immunochemical and two-dimensional gel electrophoresis characterization of cytoskeletal and noncytoskeletal compartments. Electrophoresis 15:265–277.

Renkin E (1988): "Endothelial Cell Biology in Health and Disease." Simionescu and Simionescu (eds) New York: Plenum Press, 51–68.

Rippe B, Haraldsson B (1994): Transport of macromolecules across microvascular walls: The two-pore theory. Physiol Rev 74:163–219.

Schroeder R, London E, Brown D (1994): Interactions between saturated acyl chains confer detergent resistance on lipids and glycosylphosphatidylinositol (GPI)-anchored proteins: GPI-anchored proteins in liposomes and cells show similar behavior. Proc Natl Acad Sci USA 91:12130–12134.

Sharma C, Ezzell R, Arnaout M (1995): Direct interaction of filamin (ABP-280) with β2-integrin subunit CD18. J Immunol 154:3461–3470.

Sheldon R, Moy A, Lindsley K, Shasby S, Shasby D (1993): Role of myosin light-chain phosphorylation in endothelial cell retraction. Am J Physiol 265:L606–L612.

Shepro D, Rosenthal M, Batbouta J, Roblee LS, Belamarich FA (1974): The cultivation of aortic endothelium. Anat Rec 78:523.

Shepro D (1988): Endothelial cells, inflammatory edema, and the microvascular barrier: comments by a free radical. Microvasc Res 35:247–264.

Shepro D (1994): Endothelial cytoskeletal regulation of neutrophil diapedesis. In: Physiology and Pathophysiology of Leukocyte Adhesion. New York, New York: Oxford University Press, pp. 196–216.

Smith J, Webb C, Holford J, Burgess G (1995): Signal transduction pathways for B1 and B2 bradykinin receptors in bovine pulmonary artery endothelial cells. Mol Pharmacol 17:525–534.

Sprandio J, Shapiro S, Thiagarajan P, McCord S (1988): Cultured human umbilical vein endothelial cells contain a membrane glycoprotein immunologically related to platelet glycoprotein 1b. Blood 71:234–237.

Steranka L, Farmer S, Burch R (1989): Antagonists of B2 bradykinin receptors. FASEB J 3:2019–2025.

Storrie B, Madden EA (1990): "Isolation of Subcellular Organelles. Methods in Enzymology," Vol. 182. Deutscher MP, (ed). Boston: Academic Press, Inc. pp. 203–225.

Towbin H, Staehlin T, Gordon J (1979): Electrophoretic transfer of protein from polyacrylamide cells to nitrocellulose sheets: Procedures and some applications. Proc Natl Acad Sci USA 76:4350–4354.

Walsh M (1991): Calcium-dependent mechanisms of regulation of smooth muscle contraction. Biochem Cell Biol 69:771–800.

Weihing R (1985): The filamins: Properties and functions. Can J Biochem Cell Biol 63:397–413.

Weintraub W, Negulescu P, Machen T (1992): Calcium signaling in endothelia: Cellular heterogeneity and receptor internalization. Am J Physiol 263:C1029–C1039.

Wu M, Jay D, Stracher A (1994): Existence of multiple phosphorylated forms of human platelet actin binding protein. Cell Mol Biol Res 40:351–357.

Wysolmerski R, Lagunoff D (1991): Regulation of permeabilized endothelial cell retraction by myosin phosphorylation. Am J Physiol 261:C32–C40.

Yong T, Gao X, Koizumi S, Conlon J, Rennard S, Mayhan W, Rubinstein I (1992): Role of peptidases in bradykinin-induced increase in vascular permeability in vivo. Circ Res 70:952–959.

Zhuang Q, Lawrence J, Stracher A (1988): Phosphorylation of platelet actin binding protein protects against proteolysis by calcium dependent protease. Biochem Biophys Res Commun 151:355–360.